*Molecular and Cellular Pathobiology*

Cancer Research

# Increased VEGFR-2 Gene Copy Is Associated with Chemoresistance and Shorter Survival in Patients with Non–Small-Cell Lung Carcinoma Who Receive Adjuvant Chemotherapy

Fei Yang[1,9], Ximing Tang[2], Erick Riquelme[1], Carmen Behrens[2], Monique B. Nilsson[2], Uma Giri[2], Marileila Varella-Garcia[8], Lauren A. Byers[2], Heather Y. Lin[3], Jing Wang[4], Maria G. Raso[1], Luc Girard[5], Kevin Coombes[4], J. Jack Lee[3], Roy S. Herbst[2], John D. Minna[5,6,7], John V. Heymach[2], and Ignacio I. Wistuba[1,2]

## Abstract

VEGF receptor-2 (VEGFR-2 or kinase insert domain receptor; KDR) is a known endothelial target also expressed in NSCLC tumor cells. We investigated the association between alterations in the *KDR* gene and clinical outcome in patients with resected non–small-cell lung carcinoma (NSCLC; $n = 248$). *KDR* copy number gains (CNG), measured by quantitative PCR and fluorescence *in situ* hybridization, were detected in 32% of tumors and associated with significantly higher *KDR* protein and higher microvessel density than tumors without CNGs. *KDR* CNGs were also associated with significantly increased risk of death (HR = 5.16; $P = 0.003$) in patients receiving adjuvant platinum-based chemotherapy, but no differences were observed in patients not receiving adjuvant therapy. To investigate potential mechanisms for these associations, we assessed NSCLC cell lines and found that *KDR* CNGs were significantly associated with *in vitro* resistance to platinum chemotherapy as well as increased levels of nuclear hypoxia inducible factor-1α (HIF-1α) in both NSCLC tumor specimens and cell lines. Furthermore, *KDR* knockdown experiments using small interfering RNA reduced platinum resistance, cell migration, and HIF-1α levels in cells bearing *KDR* CNGs, providing evidence for direct involvement of *KDR*. No *KDR* mutations were detected in exons 7, 11, and 21 by PCR-based sequencing; however, two variant single nucleotide polymorphism genotypes were associated with favorable overall survival in adenocarcinoma patients. Our findings suggest that tumor cell *KDR* CNGs may promote a more malignant phenotype including increased chemoresistance, angiogenesis, and HIF-1α levels, and that *KDR* CNGs may be a useful biomarker for identifying patients at high risk for recurrence after adjuvant therapy, a group that may benefit from VEGFR-2 blockade. *Cancer Res; 71(16); 5512–21. ©2011 AACR.*



## Introduction

Tumor growth is critically dependent on neovascularization (1). The ligand VEGF is an endothelial cell-specific mitogen known to be a highly potent and specific mediator of angiogenesis, and has 2 identified tyrosine kinase receptors, VEGF receptor-1 (VEGFR-1) and VEGF receptor-2 (VEGFR-2 or kinase insert domain receptor; KDR; refs. 2–5). The VEGFR-2 coded by the gene *KDR* (located in 4q12) is the predominant mediator of VEGF-stimulated endothelial cell functions, including cell migration, proliferation, survival, and enhancement of vascular permeability (6, 7). VEGFR-2 exhibits robust protein tyrosine kinase activity in response to the VEGF ligand (3).

In human epithelial tumors, including lung, VEGFR-2 has shown to be expressed in malignant cells as well as in the endothelial cell of tumor vasculature (8–11). In non–small-cell lung carcinoma (NSCLC), VEGFR-2 has been found to be overexpressed in malignant cells of tumor tissues, and

**Authors' Affiliations:** Departments of [1]Pathology, [2]Thoracic/Head and Neck Medical Oncology, [3]Biostatistics, and [4]Bioinformatics and Computational Biology, The University of Texas MD Anderson Cancer Center, Houston; [5]Hamon Center for Therapeutic Oncology; Departments of [6]Internal Medicine and [7]Pharmacology, The University of Texas Southwestern Medical Center, Dallas, Texas; [8]Department of Medicine/Medical Oncology and Pathology, University of Colorado Cancer Center, Aurora, Colorado; and [9]Department of Pathology, Shanghai Cancer Hospital, Fudan University, Shanghai, People's Republic of China

**Note:** Supplementary data for this article are available at Cancer Research Online (http://cancerres.aacrjournals.org/).

F. Yang, X. Tang, and E. Riquelme contributed equally to the work. J. V. Heymach and I. I. Wistuba are co-senior authors of this article.

**Corresponding Author:** Ignacio I. Wistuba, Department of Pathology (Unit 085), The University of Texas MD Anderson Cancer Center, 1515 Holcombe Blvd, Houston, TX 77030. Phone: 713-563-9184; Fax: 713-563-1848; E-mail: iiwistuba@mdanderson.org

**doi:** 10.1158/0008-5472.CAN-10-2614

associated with a poor outcome (8–12). The mechanism and biological impact of VEGFR-2 overexpression of NSCLC cells, however, is not known. Recent work from our group and others has shown that tumor cell expression of VEGFR-1 may drive tumor cell invasiveness (13, 14) and promote hypoxia-independent upregulation of hypoxia inducible factor-1α (HIF-1α), but it is not known whether VEGFR-2 signaling directly impacts the tumor cell phenotype in NSCLC.

Recently, a relatively high frequency (9%) of mutation and amplification of *KDR* has been detected in lung adenocarcinoma histology (15); however, the presence of these abnormalities in squamous cell carcinomas of the lung is unknown. In addition, there is no data available on the correlation of *KDR* abnormalities with tumor and patients' characteristics in lung cancer, including outcome and response to therapy.

The objective of this study was to characterize the molecular abnormalities of VEGFR-2 in epithelial malignant cells of NSCLC major histology types, adenocarcinoma and squamous cell carcinoma, and correlate with patients' clinical characteristics. We studied *KDR* copy number gain (CNG), mutation, and genetic variations in malignant cells of surgically resected NSCLC tumor tissues and correlated results with pathologic features in NSCLC patients' tumors and with their platinum adjuvant treatments and outcomes. In addition, using a series of NSCLC cell lines and tissue specimens, we investigated molecular mechanisms associated with *KDR* CNG in resistance to platinum, particularly the potential role of HIF-1α, a key regulator of angiogenesis in malignant tumors (16).

## Materials and Methods

### NSCLC tumor specimens

We obtained archived frozen and formalin-fixed and paraffin-embedded (FFPE) tissues from NSCLC patients who were surgically resected with curative intent from the Lung Cancer Specialized Program of Research Excellence (SPORE) tissue bank at The University of Texas MD Anderson Cancer Center (Houston, Texas). The tissue banking and the study were approved by the Institutional Review Board. We randomly selected 248 NSCLC specimens (159 adenocarcinomas and 89 squamous cell carcinomas) to test *KDR* abnormalities. Detailed clinical and pathologic information of the cases is presented in Supplementary Table S1.

### *KDR* copy number analysis in tumor specimens

We utilized 2 methodologies to test *KDR* CNG in NSCLC tumor specimens: real-time quantitative PCR (qPCR) and fluorescence *in situ* hybridization (FISH). To enrich for malignant cell content for qPCR analysis, tumor tissues were manually microdissected from optimal cutting temperature compound-embedded frozen tissue sections for subsequent DNA extraction. Tumor DNA was extracted using Pico Pure DNA Extraction Kit (Arcturus) according to the manufacturer's instructions. DNA samples with proportions of microdissected tumor cell greater than 70% were qualified for qPCR analysis. *KDR* gene copy number was detected by qPCR using the ABI 7300 real time PCR system (Applied Biosystems). The primers used to amplify *KDR* were KF-GACACACCCTCAGGCTCTTG and KR-ACTTTTCACCGCCT-GTTCTC. Each PCR was carried out using Power SYBR Green PCR Master Mix (Applied Biosystems) at 50°C for 2 minutes and 95°C for 10 minutes followed by 40 cycles at 95°C for 15 seconds and 60°C for 1 minute. β-Actin was introduced as the endogenous reference gene, and TaqMan Control Human Genomic DNA (Applied Biosystems) was amplified as a standard control for calibration. All sample and standard DNA reactions were set in triplicate to gauge reaction accuracy. The target gene copy number was quantified using the comparative $C_t$ method. Gene copy number of greater than 4 was considered as CNG, as previously reported (17).

*KDR* copy number analysis in NSCLC malignant tumor cells was also carried out using a dual-color FISH assay developed by 1 of the coauthors (M.V-G.). The *KDR* probe was prepared from the BAC clone RP11-21A18 obtained from CHORI. The FISH assay was conducted as we have previously published (18). Copy number analysis was done in approximately 50 nuclei per tumor in at least 4 areas. Greater than 2 gene copies per cell on average were considered as CNG.

### *KDR* copy number and VEGFR-2 and HIF-1α expression analyses in cell lines

All NSCLC cell lines were authenticated by DNA fingerprinting. Whole genome single nucleotide polymorphism (SNP) array profiling was carried out in 75 NSCLC cell lines using the Illumina Human1M-Duo DNA Analysis BeadChip (Illumina, Inc.). Prior to analysis, SNP data were normalized to the regional baseline copy number to account for aneuploidy. For VEGFR-2 reverse phase protein array (RPPA) analysis conducted in 63 NSCLC cell lines, protein lysate was collected from subconfluent cultures after 24 hours growth in media with 10% FBS and assayed by RPPA as previously described (19, 20). Cisplatin and carboplatin sensitivity was determined in triplicate by MTS (inner salt) assay for each cell line, and the concentration required for 50% growth inhibition ($IC_{50}$) was determined. For HIF-1α expression analysis, the cells were serum starved for 24 hours and stimulated with 50 ng/mL VEGF-A (R&D Systems). Cells were incubated in normoxia, and protein lysates were collected after 8 hours. HIF-1α ELISA (R&D Systems) was carried out according to the manufacturer's instructions (13).

### Microvascular density, VEGFR-2, and HIF-1α expression analyses in tumors

Histology sections were incubated with primary antibodies against VEGFR-2 (dilution 1:50; Abcam) for 90 minutes, CD34 (dilution 1:100; Lab Vision) for 35 minutes, and HIF-1α (dilution 1:100; Novus Biologicals) for 65 minutes. Tissue sections were then incubated with the secondary antibody (EnVision Dual Link+; DAKO) for 30 minutes, after which diaminobenzidine chromogen was applied for 5 minutes.

Protein expression was quantified by immunohistochemistry using light microscopy with a 200× magnification by 2 observers (F.Y. and I.W.). Tissue samples were analyzed for VEGFR-2 expression in the cytoplasm and membrane of malignant cells and for HIF-1α in the nucleus. We used a

4-value intensity score (0, 1+, 2+, and 3+) and the percentage (0% to 100%) of the extent of reactivity. The final score was obtained by multiplying the intensity and extent-of-reactivity values (range, 0–300). Microvascular density (MVD) was assessed by Ariol 2.0 Image System (Ariol, Genetix) using the criteria of Weidner and colleagues (21).

### siRNA transfection, platinum cytotoxicity, and cell migration assays in cell lines

We transfected NSCLC cells with 3 *KDR* gene-specific siRNA duplexes and control siRNA (OriGene Technology), at a final concentration of 10 nmol/L using Lipofectamine RNAiMAX (Invitrogen) according to the manufacturer's instructions. To verify the knockdown efficiency, mRNA and protein of transfected cells were collected for real-time reverse transcripatase PCR (RT-PCR) and Western blot analyses. The assessment of *in vitro* resistance to cisplatin and carboplatin was determined by the MTS assay. NSCLC cell lines were seeded in octuplicate at a density of 2,000 per well in 96-well plates. The following day, cells were treated with cisplatin and carboplatin at various concentrations ranging from 0 to 120 μmol/L for cisplatin and 0 to 200 μmol/L for carboplatin. After 72 hours of drugs exposure, 20 μL of MTS solution were added per well. Cells were incubated for 1 to 4 hours at 37°C and read at a wavelength of 490 nm. The cell migration assay using NSCLC cell lines was carried out as previously reported (13).

### *KDR* mutation and SNPs genotyping analyses

For *KDR* mutation and SNP genotyping analysis in NSCLC cell lines, we examined exons 7, 11, 21, 26, 27, and 30, using PCR-based sequencing and intron-based PCR primers as detailed in the Supplementary Table S2.

### Statistical analysis

Demographic and clinical information were compared by using the $\chi^2$ or Fisher exact tests for category variables, and Wilcoxon rank-sum or Kruskal-Wallis tests for continuous variables. The distributions of overall survival (OS) and recurrence-free survival (RFS) were estimated by the Kaplan–Meier method and compared between groups using the log-rank test. Cox proportional hazard models were used for regression analyses of survival data and conducted on OS defined as time from surgery to death or last contact, and on RFS defined as time from surgery to recurrence or last contact. Follow-up time was censored at 5 years. For the correlation analysis of *KDR* CNG in NSCLC cell lines using the whole genome SNP arrays data with cisplatin sensitivity, we used the Wilcoxon rank sum test. The NSCLC cell lines RPPA data were quantified using the SuperCurve method which detects changes in protein level as previously reported (22).

## Results

### *KDR* gene CNG analysis

In epithelial malignant NSCLC cells microdissected from tumor tissues, *KDR* CNG was detected in 45 (32%) of 139 tumors examined. Similar frequency of *KDR* CNG was found in adenocarcinoma (26/85, 31%) and squamous cell carcinoma (19/54, 35%) histologies ($P = 0.572$). The range of increased *KDR* copy numbers was from 4 to 11 gene copies. None of 15 normal tissue samples adjacent to the NSCLC tested showed *KDR* CNG. To confirm *KDR* CNG results by qPCR, 20 tumor specimens with *KDR* CNG by qPCR were examined by FISH. *KDR* copy gains in the malignant cells were confirmed by FISH in all 20 NSCLC specimens detected by qPCR (Fig. 1A).

### Correlation between *KDR* CNG and VEGFR-2 protein expression and MVD

To assess the immunohistochemical (IHC) expression of VEGFR-2 in NSCLC malignant cells and the MVD (CD34) in lung tumor tissue stroma, we selected 52 lung tumor specimens with whole histologic sections from FFPE tissues. Of these, 26 cases had *KDR* CNG and 26 cases did not. VEGFR-2 protein expression was present both in the cytoplasm and membrane of malignant cells as well as in vessel endothelial cells (Fig. 1B).

Levels of VEGFR-2 expression in cytoplasm and in membrane were associated with *KDR* CNG in malignant cells of NSCLC. Tumors with *KDR* CNG showed significantly higher cytoplasmic ($P = 0.013$) and membrane ($P = 0.009$) VEGFR-2 protein expression in the malignant cells (Fig. 1C), and higher MVD ($P = 0.018$) and larger vessel areas ($P = 0.033$) in the tumor stroma than cases without *KDR* CNG (Fig. 2A and B).

### Association between tumor *KDR* CNG, clinicopathologic features, and clinical outcome

When we correlated *KDR* CNG with patients' clinicopathologic features, we did not find correlation with tumor histology, smoking status, and tumor stage. In the multivariate analysis after adjusting for stage and adjuvant therapy, *KDR* CNG was associated with poor OS (HR = 4.0; 95% CI: 1.76–9.07; $P = 0.001$) and shortened RFS (HR = 1.83, 95% CI: 1.02–3.29; $P = 0.044$) in 115 NSCLC patients who underwent surgical resection. Strikingly, *KDR* CNG was associated with a significantly worse OS (HR = 5.16, 95% CI: 1.75–15.2; $P = 0.003$) in NSCLC patients receiving platinum adjuvant therapy, but not in patients without adjuvant therapy ($P = 0.349$; Fig. 3 and Table 1). These data suggest that *KDR* CNG in malignant cells may represent a predictive marker of worse outcome in patients with surgically resected NSCLC treated with platinum-based adjuvant chemotherapy.

We also investigated and examined the impact of neoadjuvant chemotherapy on *KDR* CNGs. The platinum neoadjuvant-treated tumors (33%, 8/24) had similar frequency of *KDR* CNGs than cases without neoadjuvant therapy (32%, 37/115).

### *KDR* CNG and VEGFR-2 protein levels and correlation with platinum resistance in cell lines

The association detected between *KDR* CNG and worse outcome in patients treated with platinum adjuvant therapy prompted us to examine the correlation between *KDR* gain and VEGFR-2 protein levels in NSCLC cell lines with *in vitro* resistance to platinum drugs. *KDR* CNG was assessed by SNP array analysis in 75 NSCLC cell lines. Cell lines with *KDR* copy gains of 6 to 9 copies or 10 or more copies above the regional baseline copy number were identified. Nineteen (25%) cell

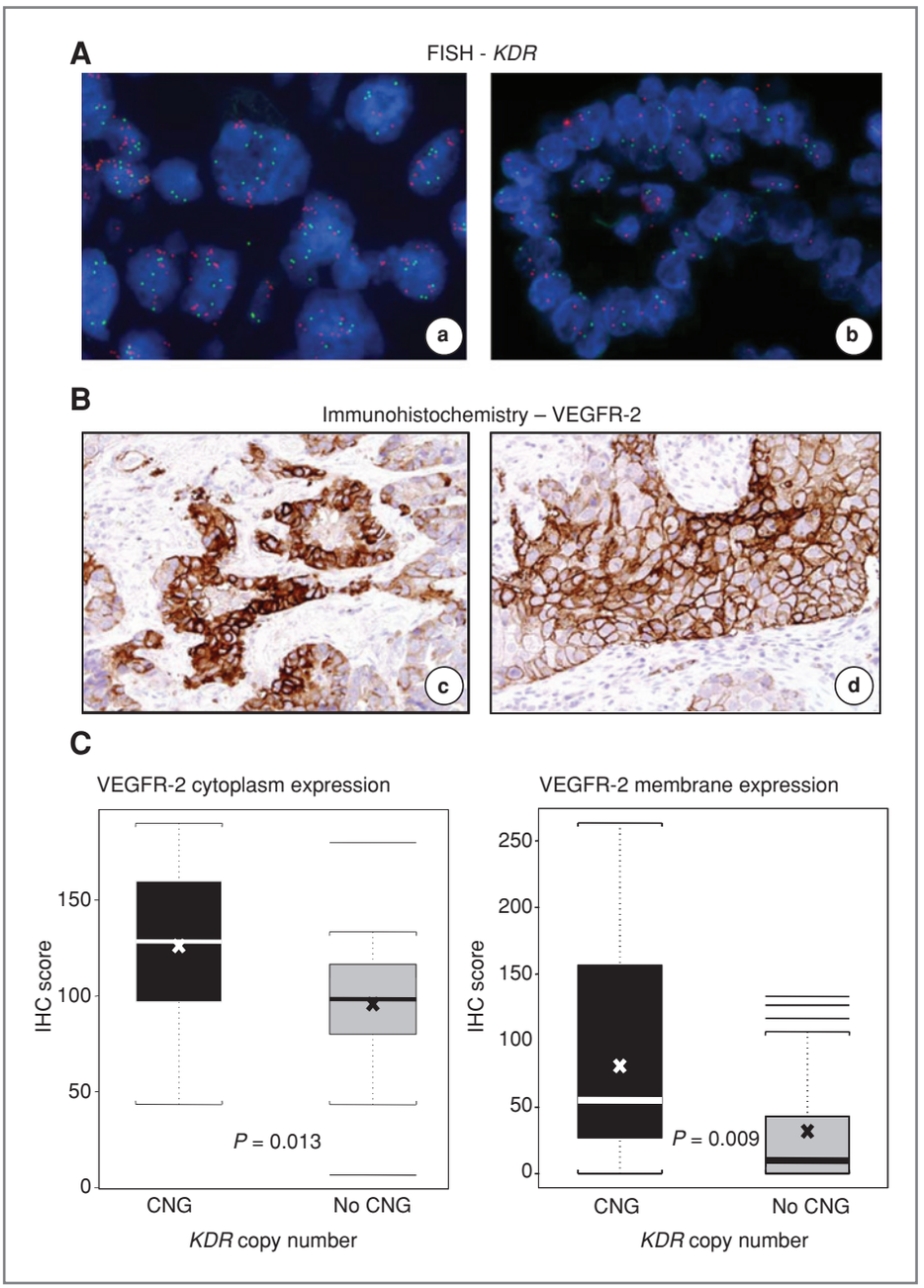


**Figure 1.** *KDR* CNG correlated with VEGFR-2 protein expression in NSCLC tumors. A, representative examples of *KDR* copy number examined by FISH in NSCLC tissue specimens. a, CNG; b, no CNG. Red signals represent the *KDR* gene probe, and green signals the internal control probe (magnification 1,000×). B, representative example of IHC expression of VEGFR-2 in NSCLC tissue specimens. VEGFR-2 protein expression was present both in the cytoplasm and membrane of tumor cells in (c) adenocarcinoma and (d) squamous cell carcinoma (magnification 200×). C, expression of VEGFR-2 in tumors with *KDR* CNG compared with lung cancers without CNG. The box plots depict scores of IHC expression of VEGFR-2 cytoplasm and VEGFR-2 membrane comparing 26 lung cancers having *KDR* CNG with 26 lung cancers without CNG. In the box plots, bars indicate median score, *x* indicates mean scores, and dashed line SD.

lines showed *KDR* CNG defined as 6 or more copies. Of these, 3 (4%) cell lines contained high-level gains (≥10 copies), and 16 (21%) had CNG between 6 to 9. Of interest, cisplatin sensitivity in cell lines with 6 or more *KDR* copies showed significantly more resistance to cisplatin ($P = 0.0179$; Fig. 4A).

Then, we correlated the expression of VEGFR-2 protein in a panel of 63 untreated NSCLC cell lines by RPPA with each cell line's sensitivity to cisplatin or carboplatin. We found that higher VEGFR-2 expression levels were significantly associated with resistance to both cisplatin (Fig. 4B) and carboplatin (data not shown) by Pearson correlation. The correlation coefficient ($r$) between VEGFR-2 expression and the concentration of cisplatin and carboplatin required to inhibit cell growth by 50% ($IC_{50}$) were 0.346 ($P = 0.005$) and 0.319 ($P = 0.011$), respectively.

### Effect of *KDR* knockdown on platinum sensitivity and cell migration in cell lines

To investigate the role of *KDR* CNG and VEGFR-2 overexpression in resistance to both cisplatin and carboplatin, we

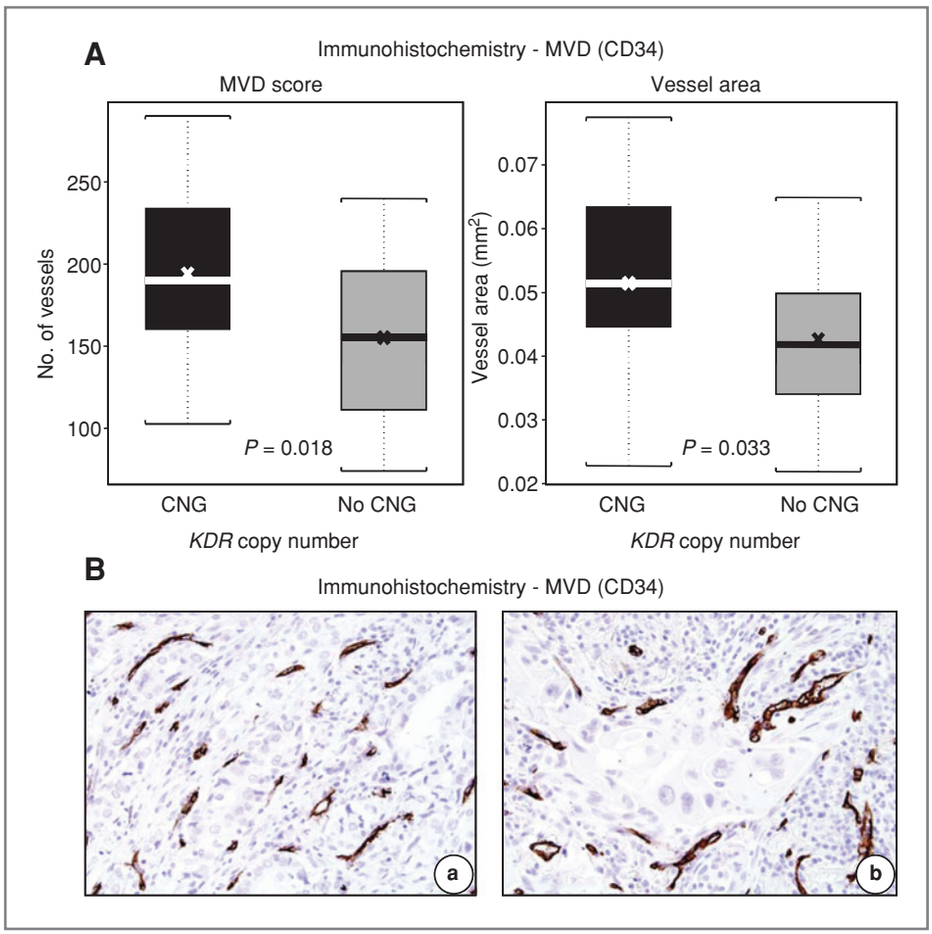


**Figure 2.** *KDR* CNG correlated with MVD in NSCLC tumors. A, expression of MVD in tumors with *KDR* CNG compared with lung cancers without CNG. The box plots depict scores of IHC assessment of MVD and vessel area ($mm^2$) comparing tumors with and without *KDR* CNG. In the box plots, bars indicate median score, *x* indicates mean scores, and dashed line SD. B, representative example of IHC expression of CD34-positive vessels (MVD) in (a) adenocarcinoma and (b) squamous cell carcinoma (magnification 200×).

utilized siRNA to knock down *KDR* expression in H23 and H461 NSCLC cell lines, which contain 6 to 9 *KDR* gene copies, and as control A549 NSCLC cell line with normal *KDR* copy number. In both cell lines, siRNA targeting *KDR* significantly decreased *KDR* mRNA expression by real-time RT-PCR, and VEGFR-2 expression by Western blot, compared with control cells transfected with scrambled siRNA and nontransfected cells ($P < 0.05$; Fig. 4C). The *in vitro* sensitivity of H23 and H461 cells to cisplatin (Fig. 4D) or carboplatin (data not shown) treatment was increased in si*KDR* transfected cells compared with control siRNA-transfected or untransfected cells, suggesting that VEGFR-2 is contributing to chemoresistance in this model. This phenomenon was not observed in cell A549 with normal *KDR* copy number.

In addition, we found that knockdown of reduction of VEGFR-2 expression induced by si*KDR* transfection significantly inhibited the migration of H23 and H461 cells compared with siRNA control-transfected or untransfected cells (Fig. 4E and F).

### Correlation between *KDR* CNG and HIF-1α expression in cell lines and tumors

The observations that *KDR* CNGs were associated with increased angiogenesis, chemoresistance, and migration suggested that VEGFR-2 may be impacting the HIF-1α pathway, which is known to impact each of these cellular properties (13, 14). To investigate this further, we evaluated HIF-1α levels by ELISA in a panel of NSCLC cell lines with a range of *KDR* copy numbers and expression of VEGFR-2. HIF-1α levels were higher in cell lines with *KDR* CNG, and significantly ($P = 0.02$) higher in cells with 6 to 9 gene copies, compared with cells with no CNG (Fig. 5A). In H23 cells which have *KDR* CNG, stimulation with 50 ng/mL VEGF-A for 8 hours induced a rise in HIF-1α expression. Furthermore, knockdown of *KDR* with siRNA significantly ($P = 0.01$) reduced HIF-1α levels (Fig. 5B). This phenomenon was not detected in cell lines A549 with normal *KDR* copy number. These data indicated that VEGFR-2 can regulate HIF-1α in a ligand-dependent, but hypoxia-independent, manner in NSCLC cells.

We next investigated the potential association between *KDR* CNG and HIF-1α in NSCLC clinical specimens. Similar to the results in the NSCLC cell lines, tumor tissue specimens with *KDR* CNG ($n = 25$) showed a significantly ($P = 0.037$) higher expression of nuclear HIF-1α expression by immunohistochemistry than tumors without CNG ($n = 22$; Fig. 5C and D).

### *KDR* mutation and SNP analyses

To investigate whether alterations in the *KDR* gene other than CNGs may impact NSCLC tumors, we assessed the *KDR*

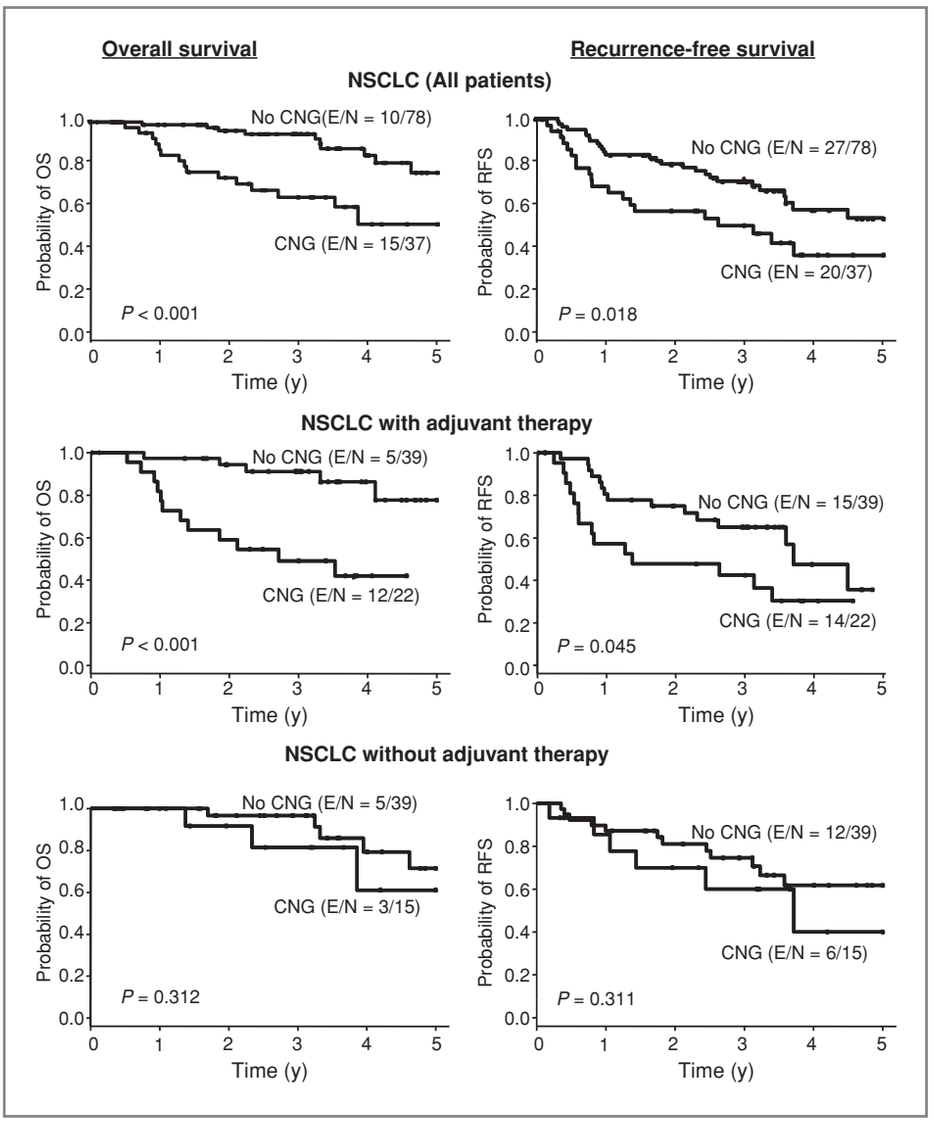


**Figure 3.** *KDR* CNG associated with outcome in NSCLC patients treated with adjuvant chemotherapy. Kaplan–Meier curve for OS and RFS by *KDR* CNG in NSCLC patients and 2 subgroups of platinum adjuvant therapy and without adjuvant therapy (E, event; N, total number of cases).

gene for mutations and SNPs. For *KDR* mutation analysis in NSCLC cell lines, we examined 6 *KDR* exons (7, 11, 21, 26, 27 and 30) they showed to be mutant in adenocarcinoma tumors in a study published by Ding and colleagues (15). In 37 tested NSCLC cell lines, we found only 2 mutations in the *KDR* gene, an intronic T + 2A exon 11 mutation in HCC2450 and a

**Table 1.** Multivariate analysis for outcome by *KDR* copy gain in NSCLC patients by adjuvant chemotherapy

| Cases | *N* | Comparison | Outcome | Adjusted HR[a] (95% CI) | *P* |
|---|---|---|---|---|---|
| All patients | 115 | Gain vs. no gain | OS | 4.00 (1.76–9.07) | 0.001 |
| | | | RFS | 1.83 (1.02–3.29) | 0.044 |
| Adjuvant therapy | 61 | Gain vs. no gain | OS | 5.16 (1.75–15.2) | 0.003 |
| | | | RFS | 1.87 (0.9–3.92) | 0.1 |
| No adjuvant therapy | 54 | Gain vs. no gain | OS | 1.99 (0.47–8.4) | 0.349 |
| | | | RFS | 1.83 (0.66–5.05) | 0.243 |

[a]Adjusting for tumor stage; follow-up is censored at 5 years.

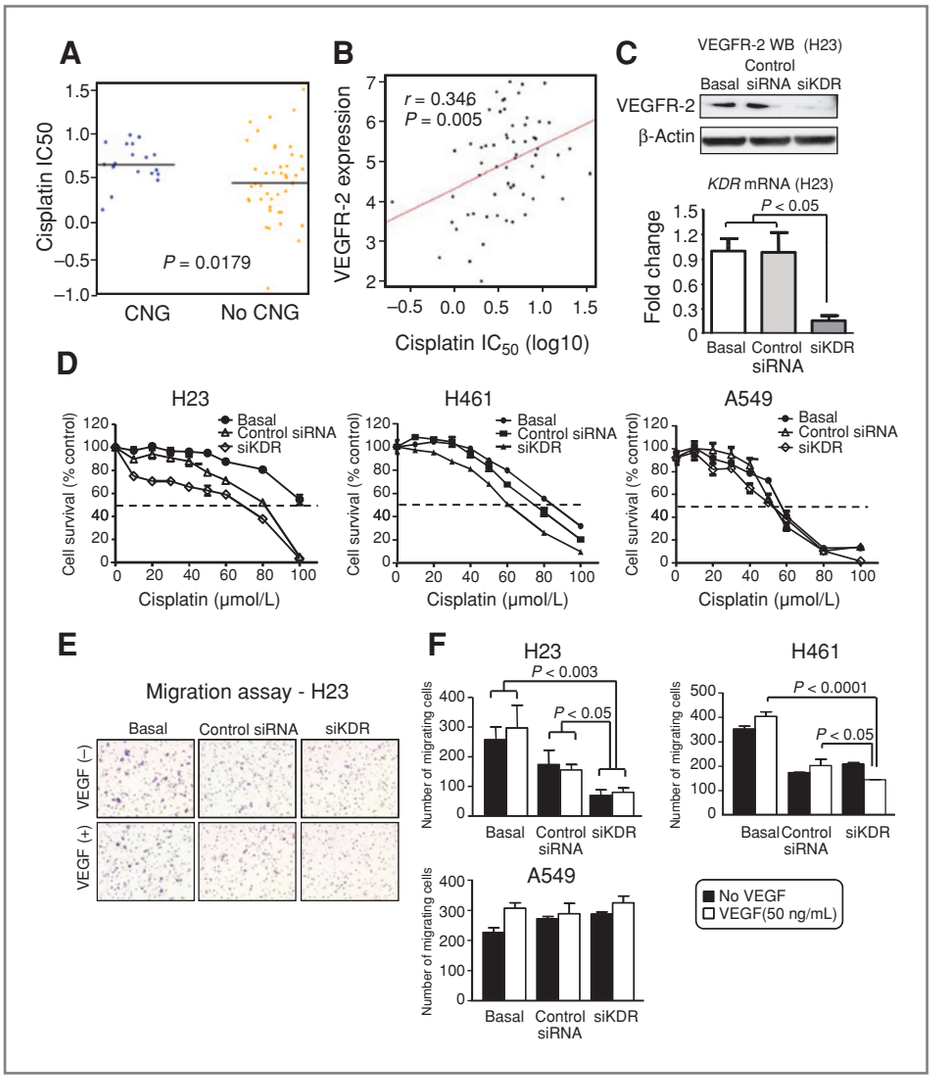


**Figure 4.** *KDR* CNG and VEGFR-2 expression associated with resistance to cisplatin. A, correlation of *KDR* CNG with *in vitro* resistance to cisplatin. NSCLC cell lines showing CNG (≥6 copies) showed significantly higher $IC_{50}$ compared with cell lines without CNG. B, correlation between the concentrations of cisplatin required to inhibit NSCLC cell growth ($IC_{50}$) and VEGFR-2 protein expression levels by RPPA. C, si*KDR* in NSCLC cell line H23 inhibited significantly the expression of VEGFR-2 by Western blot (WB) and *KDR* mRNA by qRT-PCR compared with basal and scrambled control siRNA (bars, SD). D, knocking down *KDR* using siRNA decreased the viability of NSCLC cell lines H23 and H461 (6–9 copies) exposed to cisplatin by MTS assay (data are graphed as mean percent increase ± percent SD). Knockdown of *KDR* in H23 cells caused 1.9-fold decrease in the cisplatin $IC_{50}$ ($P < 0.05$) and 3.5-fold decrease in the carboplatin $IC_{50}$ ($P < 0.05$). Knockdown of *KDR* in H461 cells caused 1.3-fold decrease in the cisplatin $IC_{50}$ ($P < 0.05$). Knockdown of *KDR* in A549 cells did not decrease cisplatin or carboplatin $IC_{50}$. E, migration of NSCLC cell line H23 by Boyden chamber assay was inhibited by si*KDR* in cells with and without stimulation with VEGF. F, quantification of the migration assay of NSCLC cell lines before and after knocking down *KDR* using si*KDR* in cells with and without stimulation with VEGF showed decreased migration in H23 and H461 cells (6–9 *KDR* copies), but not in A549 cells (*KDR* no CNG; bars, SD).

CGT946CAT point mutation in exon 21 in HCC2279. No mutation affecting exons 11 and 21 was detected in 200 NSCLC tissues specimens examined.

In addition, 3 *KDR* SNPs (889G/A, 1416A/T, and -37A/G) were genotyped in DNA extracted from 200 NSCLC tumors (Supplementary Table S3), and correlated with patients clinicopathologic features, including outcome. We did not find correlation between the SNP genotypes distribution and OS or RFS of all NSCLC patients examined. In adenocarcinoma patients both *KDR* 1416 AT/TT (HR = 0.45, 95% CI: 0.2–0.99; $P = 0.048$) and -37AG/GG (HR = 0.43, 95% CI: 0.2–0.92; $P = 0.031$) variant genotypes were associated with a favorable OS in the multivariate analysis after adjusting for tumor stage and neoadjuvant therapy (Supplementary Fig. S1, and Supplementary Table S4).

Furthermore, among NSCLC patients with the *KDR* 889 GA/AA variant genotypes, those who received platinum neoadjuvant and/or adjuvant chemotherapy showed a significantly better OS (HR = 0.22, 95% CI: 0.05–0.94; $P = 0.041$) than patients who did not receive chemotherapy in the multivariate

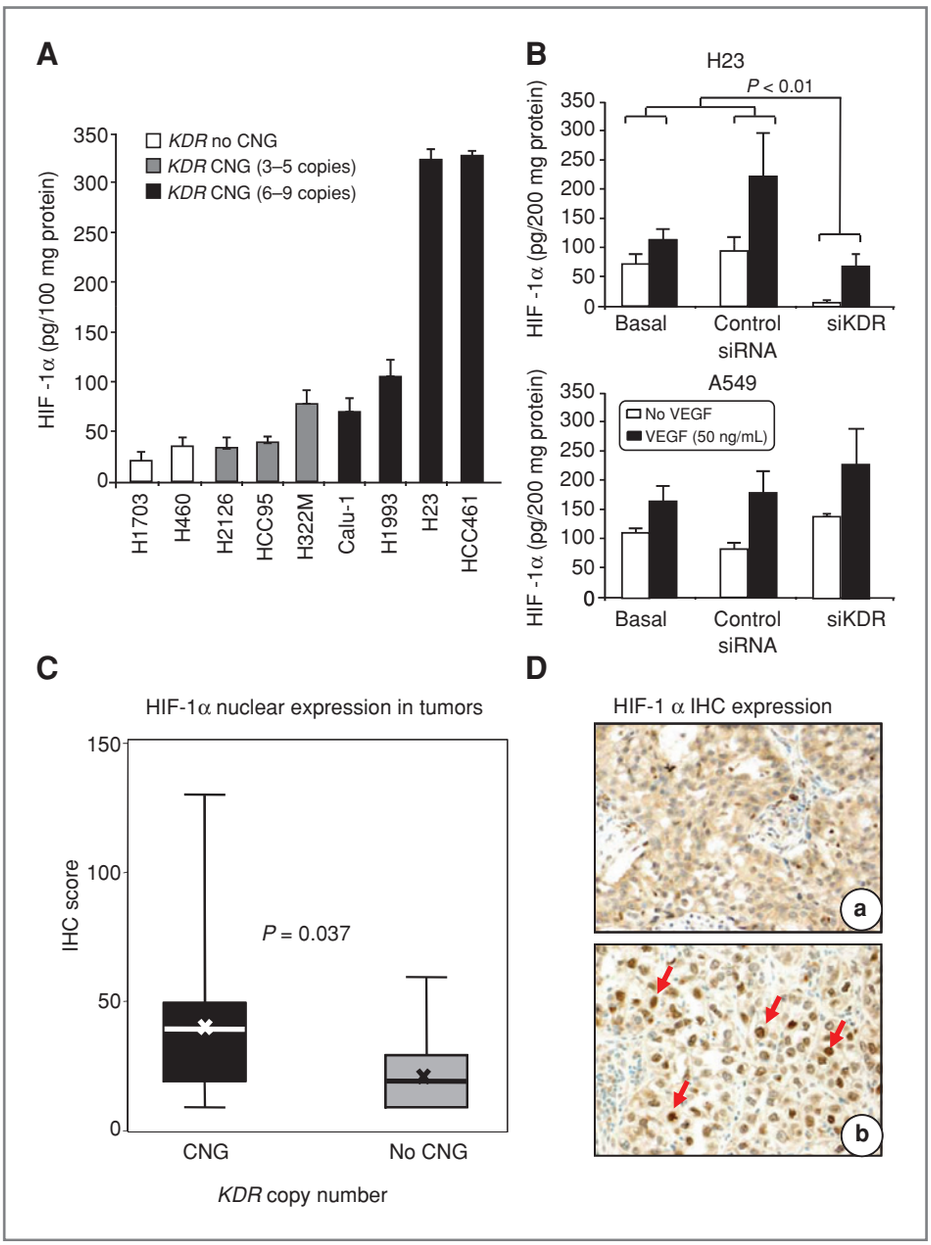


**Figure 5.** *KDR* CNG correlated with HIF-1α expression in NSCLC cell lines and tumor tissue specimens. A, HIF-1α protein expression determined by ELISA correlated with *KDR* CNG in a series of NSCLC cell lines (bars, SD; cell lines with CNG 6–9 copies versus 3–5 copies and no CNG, $P < 0.02$). B, HIF-1α expression by ELISA was markedly inhibited by knocking down using si*KDR* in NSCLC H23 cell line, but not in A549 cell line, with and without stimulation with VEGF (bars, SD). C, expression of nuclear HIF-1α in tumors with *KDR* CNG compared with lung cancers without CNG. The box plots depict scores of IHC expression of nuclear HIF-1α comparing 22 lung cancers having *KDR* CNG with 25 lung cancers without CNG. In the box plots, bars indicate median score, *x* indicates mean scores, and dashed line standard deviation. D, representative example of low (a, adenocarcinoma) and high (b, squamous cell carcinoma) IHC expression of HIF-1α in NSCLC tissue specimens (magnification 200×). Red arrows, positive nuclear HIF-1α immunostaining.

analysis after adjusting for histology and tumor stage. However, no survival benefit was found in NSCLC patients with *KDR* 889 GG wild genotype (HR = 1.23, 95% CI: 0.64–2.35; $P = 0.538$).

## Discussion

Our study represents the first report in lung cancer showing a high frequency of *KDR* CNG (32%) in both major histology types of NSCLC, adenocarcinoma, and squamous cell carcinoma, by qPCR and confirmed in a subset of cases by FISH. Notably, *KDR* CNG predicted worse OS in patients who received platinum adjuvant therapy but not in untreated patients. In NSCLC cell lines, we found that *KDR* CNGs were significantly associated with *in vitro* resistance to platinum chemotherapy, as well as increased levels of nuclear HIF-1α. Furthermore, *KDR* knockdown experiments using siRNA reduced platinum resistance, cell migration, and HIF-1α levels in cells bearing *KDR* CNGs, providing evidence for direct involvement of *KDR*. Our findings suggest that tumor cell *KDR* CNGs may promote a more malignant phenotype including increased chemoresistance, angiogenesis, and HIF-1α levels.

In our study, tumors with *KDR* CNG in the malignant cells showed significantly higher VEGFR-2 protein expression in the cytoplasm and membrane of those cells, as well as higher MVD and larger vessel areas in the tumor stroma, compared

with tumors lacking the *KDR* CNG. One possible explanation for this association is that tumor cell VEGFR-2 binds circulating VEGF, increasing local concentrations of the ligand which in turn increases angiogenesis through effects on tumor endothelium. Another possible explanation is that VEGFR-2 overexpressing lung cancer cells may express increased levels of VEGF and other proangiogenic factors via upregulation of HIF-1α, which in turn could promote autocrine or paracrine signaling that further increases expression. These mechanisms are not mutually exclusive and merit further investigation. Our finding of correlations between *KDR* CNG and higher expression of HIF-1α in NSCLC cell lines and tumor specimens support the latter hypothesis. It has been showed that activation of several receptor tyrosine kinases (RTK; RET, VEGFR-1, epidermel growth factor receptor, and platelet-derived growth factor receptor) increases HIF-1α levels in a cell-specific manner in tumors (13, 23, 24); therefore, our data represent the first evidence suggesting that VEGFR-2 may be another RTK that plays a role in increasing the levels of HIF-1α expression in cancer.

A provocative finding of this study is this first report that *KDR* CNG in malignant cells predicted a worse outcome of NSCLC patients receiving platinum adjuvant chemotherapy after surgical resection with curative intent, but was not predictive in patients without adjuvant therapy. These findings suggest that *KDR* CNG may represent a potential biomarker for predicting resistance to adjuvant platinum-based chemotherapy in NSCLC patients. It is also noteworthy that VEGFR-2 knockdown reduced chemoresistance and cell migration, and lowered HIF-1α levels, using *in vitro* NSCLC models. One potential implication of these findings is that VEGFR-2 blockade may sensitize tumors bearing *KDR* CNGs to chemotherapy directly through effects of the tumor cells themselves, in addition to its effect on tumor endothelial cells. *KDR* CNGs may therefore identify a group of NSCLC patients that would receive greater relative benefit from combinations of VEGF pathway inhibitors with chemotherapy than patients lacking *KDR* CNGs. Further prospective studies with larger patient cohorts are needed to assess the role of *KDR* CNG in NSCLC tumors and outcome of NSCLC patients treated with platinum-based chemotherapy in both surgically resected and advanced metastatic tumor settings, and to determine whether *KDR* CNGs are predictive of either chemoresistance or benefit for VEGF inhibitor benefit/chemotherapy combinations compared with chemotherapy alone.

Our finding that *KDR* CNG by SNP array and higher levels of VEGFR-2 expression by RPPA in a large series of NSCLC cell lines correlated significantly with *in vitro* resistance to platinum dugs (cisplatin for *KDR* CNG, and cisplatin and carboplatin for VEGFR-2 expression) provides support to our clinical observation. The increased sensitivity of the NSCLC cell lines having *KDR* CNG to *in vitro* treatment with cisplatin or carboplatin after inhibition of *KDR* mRNA and protein expressions further supports the concept that *KDR* CNG may promote platinum resistance in NSCLC. Although the exact mechanism needs to be elucidated, we postulate that the increased expression of HIF-1α induced by *KDR* CNG, and subsequent VEGFR-2 expression, in malignant NSCLC cells may explain increased platinum resistance in NSCLC. Interestingly, HIF-1α has been previously associated to chemoresistance in NSCLC (25, 26) and other solid tumor types (27, 28).

The finding that inhibition of *KDR* and VEGFR-2 expression resulted in decreased NSCLC cell migration points out another new interesting role of VEGFR-2 in NSCLC malignant cells. It has been established that, among other functions, VEGFR-2 is an important mediator of VEGF-stimulated endothelial cell migration (29, 30). We have also observed that that HIF-1α mediates migration driven by another RTK, EGFR, in NSCLC, independent of hypoxia (31).

In our study, the variant genotypes of *KDR* SNPs 1416 (AT/TT) and -37(AG/GG) associated with a favorable OS in the multivariate analysis. Ours is the first report showing association between *KDR* SNP genotypes and prognosis in lung cancer. In breast cancer patients, the *KDR* SNP 1416 A/T genotypic variant was associated with the expression of progesterone receptors, and its presence suggested a better prognosis for carriers of the *T* allele (32). Questions remain about the functional roles of the *KDR* SNPs responsible for the associations with outcome of NSCLC patients, particularly in adenocarcinoma patients, found in our study.

In summary, our findings indicate that *KDR* CNG was frequently detected in NSCLC tumors and associated with platinum resistance *in vivo* and *in vitro*, and may be a useful biomarker for identifying patients at high risk for recurrence after adjuvant therapy, a group that may benefit from VEGFR-2 blockade.

## Disclosure of Potential Conflicts of Interest

No potential conflicts of interest were disclosed.

## Grant Support

This study was supported by grants from the Department of Defense (W81XWH-07-1-0306 to J.D. Minna, J.V. Heymach, and I.I. Wistuba), the Specialized Program of Research Excellence in Lung Cancer (P50CA70907 to J.D. Minna, J.V. Heymach, and I.I. Wistuba; P50CA58187 to M. Varella-Garcia), and the National Cancer Institute (Cancer Center Support Grant CA-16672).

The costs of publication of this article were defrayed in part by the payment of page charges. This article must therefore be hereby marked *advertisement* in accordance with 18 U.S.C. Section 1734 solely to indicate this fact.

Received July 18, 2010; revised June 2, 2011; accepted June 26, 2011; published OnlineFirst July 1, 2011.

## References

1. Folkman J. Tumor angiogenesis: therapeutic implications. N Engl J Med 1971;285:1182–6.
2. Fidler IJ, Ellis LM. The implications of angiogenesis for the biology and therapy of cancer metastasis. Cell 1994;79:185–8.
3. Waltenberger J, Claesson-Welsh L, Siegbahn A, Shibuya M, Heldin CH. Different signal transduction properties of KDR and Flt1, two receptors for vascular endothelial growth factor. J Biol Chem 1994;269:26988–95.

4. Ferrara N, Davis-Smyth T. The biology of vascular endothelial growth factor. Endocr Rev 1997;18:4–25.
5. Hanahan D, Weinberg RA. Hallmarks of cancer: the next generation. Cell 2011;144:646–74.
6. Terman BI, Carrion ME, Kovacs E, Rasmussen BA, Eddy RL, Shows TB. Identification of a new endothelial cell growth factor receptor tyrosine kinase. Oncogene 1991;6:1677–83.
7. Bernatchez PN, Soker S, Sirois MG. Vascular endothelial growth factor effect on endothelial cell proliferation, migration, and platelet-activating factor synthesis is Flk-1-dependent. J Biol Chem 1999;274:31047–54.
8. Ishii H, Yazawa T, Sato H, Suzuki T, Ikeda M, Hayashi Y, et al. Enhancement of pleural dissemination and lymph node metastasis of intrathoracic lung cancer cells by vascular endothelial growth factors (VEGFs). Lung Cancer 2004;45:325–37.
9. Ludovini V, Gregorc V, Pistola L, Mihaylova Z, Floriani I, Darwish S, et al. Vascular endothelial growth factor, p53, Rb, Bcl-2 expression and response to chemotherapy in advanced non-small cell lung cancer. Lung Cancer 2004;46:77–85.
10. Seto T, Higashiyama M, Funai H, Imamura F, Uematsu K, Seki N, et al. Prognostic value of expression of vascular endothelial growth factor and its flt-1 and KDR receptors in stage I non-small-cell lung cancer. Lung Cancer 2006;53:91–6.
11. Carrillo de Santa Pau E, Arias FC, Caso Pelaez E, Munoz Molina GM, Sanchez Hernandez I, Muguruza Trueba I, et al. Prognostic significance of the expression of vascular endothelial growth factors A, B, C, and D and their receptors R1, R2, and R3 in patients with nonsmall cell lung cancer. Cancer 2009;115:1701–12.
12. Donnem T, Al-Saad S, Al-Shibli K, Delghandi MP, Persson M, Nilsen MN, et al. Inverse prognostic impact of angiogenic marker expression in tumor cells versus stromal cells in non small cell lung cancer. Clin Cancer Res 2007;13:6649–57.
13. Nilsson MB, Zage PE, Zeng L, Xu L, Cascone T, Wu HK, et al. Multiple receptor tyrosine kinases regulate HIF-1alpha and HIF-2alpha in normoxia and hypoxia in neuroblastoma: implications for antiangiogenic mechanisms of multikinase inhibitors. Oncogene 2010;29:2938–49.
14. Roybal JD, Zang Y, Ahn YH, Yang Y, Gibbons DL, Baird BN, et al. miR-200 Inhibits lung adenocarcinoma cell invasion and metastasis by targeting Flt1/VEGFR1. Mol Cancer Res 2010;9:25–35.
15. Ding L, Getz G, Wheeler DA, Mardis ER, McLellan MD, Cibulskis K, et al. Somatic mutations affect key pathways in lung adenocarcinoma. Nature 2008;455:1069–75.
16. Du R, Lu KV, Petritsch C, Liu P, Ganss R, Passegue E, et al. HIF1alpha induces the recruitment of bone marrow-derived vascular modulatory cells to regulate tumor angiogenesis and invasion. Cancer Cell 2008;13:206–20.
17. Yamamoto H, Shigematsu H, Nomura M, Lockwood WW, Sato M, Okumura N, et al. PIK3CA mutations and copy number gains in human lung cancers. Cancer Res 2008;68:6913–21.
18. Tang X, Kadara H, Behrens C, Liu DD, Xiao Y, Rice D, et al. Abnormalities of the TITF-1 lineage-specific oncogenes in NSCLC: implications in lung cancer pathogenesis and prognosis. Clin Cancer Res 2011;17:2434–43.
19. Cheng KW, Lu Y, Mills GB. Assay of Rab25 function in ovarian and breast cancers. Methods Enzymol 2005;403:202–15.
20. Byers LA, Sen B, Saigal B, Diao L, Wang J, Nanjundan M, et al. Reciprocal regulation of c-Src and STAT3 in non-small cell lung cancer. Clin Cancer Res 2009;15:6852–61.
21. Weidner N, Semple JP, Welch WR, Folkman J. Tumor angiogenesis and metastasis–correlation in invasive breast carcinoma. N Engl J Med 1991;324:1–8.
22. Hu J, He X, Baggerly KA, Coombes KR, Hennessy BT, Mills GB. Non-parametric quantification of protein lysate arrays. Bioinformatics 2007;23:1986–94.
23. Hirami Y, Aoe M, Tsukuda K, Hara F, Otani Y, Koshimune R, et al. Relation of epidermal growth factor receptor, phosphorylated-Akt, and hypoxia-inducible factor-1alpha in non-small cell lung cancers. Cancer Lett 2004;214:157–64.
24. Phillips RJ, Mestas J, Gharaee-Kermani M, Burdick MD, Sica A, Belperio JA, et al. Epidermal growth factor and hypoxia-induced expression of CXC chemokine receptor 4 on non-small cell lung cancer cells is regulated by the phosphatidylinositol 3-kinase/PTEN/AKT/mammalian target of rapamycin signaling pathway and activation of hypoxia inducible factor-1alpha. J Biol Chem 2005;280:22473–81.
25. Mi J, Zhang X, Rabbani ZN, Liu Y, Reddy SK, Su Z, et al. RNA aptamer-targeted inhibition of NF-kappa B suppresses non-small cell lung cancer resistance to doxorubicin. Mol Ther 2008;16:66–73.
26. Wen W, Ding J, Sun W, Wu K, Ning B, Gong W, et al. Suppression of cyclin D1 by hypoxia-inducible factor-1 via direct mechanism inhibits the proliferation and 5-fluorouracil-induced apoptosis of A549 cells. Cancer Res 2010;70:2010–9.
27. Koukourakis MI, Giatromanolaki A, Sivridis E, Simopoulos C, Turley H, Talks K, et al. Hypoxia-inducible factor (HIF1A and HIF2A), angiogenesis, and chemoradiotherapy outcome of squamous cell head-and-neck cancer. Int J Radiat Oncol Biol Phys 2002;53:1192–202.
28. Tan EY, Yan M, Campo L, Han C, Takano E, Turley H, et al. The key hypoxia regulated gene CAIX is upregulated in basal-like breast tumours and is associated with resistance to chemotherapy. Br J Cancer 2009;100:405–11.
29. Rousseau S, Houle F, Landry J, Huot J. p38 MAP kinase activation by vascular endothelial growth factor mediates actin reorganization and cell migration in human endothelial cells. Oncogene 1997;15:2169–77.
30. Qi JH, Claesson-Welsh L. VEGF-induced activation of phosphoinositide 3-kinase is dependent on focal adhesion kinase. Exp Cell Res 2001;263:173–82.
31. Xu L, Nilsson MB, Saintigny P, Cascone T, Herynk MH, Du Z, et al. Epidermal growth factor receptor regulates MET levels and invasiveness through hypoxia-inducible factor-1alpha in non-small cell lung cancer cells. Oncogene 2010;29:2616–27.
32. Forsti A, Jin Q, Altieri A, Johansson R, Wagner K, Enquist K, et al. Polymorphisms in the KDR and POSTN genes: association with breast cancer susceptibility and prognosis. Breast Cancer Res Treat 2007;101:83–93.